

Engineering Notes

ENGINEERING NOTES are short manuscripts describing new developments or important results of a preliminary nature. These Notes cannot exceed 6 manuscript pages and 3 figures; a page of text may be substituted for a figure and vice versa. After informal review by the editors, they may be published within a few months of the date of receipt. Style requirements are the same as for regular contributions (see inside back cover).

Fickle Effect of Nose Microasymmetry on the High-Alpha Aerodynamics

Lars E. Ericsson*

Lockheed Missiles & Space Company, Inc.,
Sunnyvale, California 94088

Introduction

IN a recent publication¹ it was shown that the widely differing yawing moment variation with sideslip of a slender-nose vehicle²⁻⁴ (Fig. 1) could be related to the well-known side-force sensitivity to roll angle^{1,2} (Fig. 2) when using the total-angle-of-attack concept. In this manner, by using the ϕ - β equivalence, the experimental results in Fig. 2 generated the side-force characteristics shown in Fig. 3. The nonuniqueness of the $C_Y(\beta)$ curves was obtained by shifting the $C_Y(\phi)$ curves in Fig. 2 by the ϕ values shown in Fig. 3. These shifts would simply represent possible biases generated by nose microasymmetry on wind-tunnel models. The experimental results of the yawing moment C_n as a function of sideslip β obtained by others^{3,4} for a 3.5-caliber ogive could be predicted using the $C_n(\beta)$ family of curves corresponding to Fig. 3.

Discussion

If one assumes that at high angles of attack the lateral stability characteristics of an aircraft are dominated by the asymmetric loads generated on a slender forebody, which is what experimental results^{5,6} indicate, one can use body-alone characteristics at high alpha. Consequently, representing the slender nose of a tested F-111 aircraft model⁷ by an ogive cylinder, the maximum contribution of the forebody to the yawing moment was estimated¹ (Fig. 4). It can be seen that the $C_n(\beta)$ characteristics at large sideslip, $|\beta| > 10$ deg, are well predicted in this manner. The switch of the asymmetry occurred near zero yaw in the test, but could, according to Fig. 3, occur at any angle in the range -20 deg $\leq \beta \leq 20$ deg.

Based on this ϕ - β data correlation and the demonstrated possible variations in $C_Y(\beta)$ and $C_n(\beta)$ characteristics for aircraft with long slender noses, the characteristics shown in Fig. 5 were presented in Ref. 1 as equally possible forms of the $C_Y(\beta)$ and $C_n(\beta)$ characteristics of advanced aircraft. The following testing procedure was suggested: "The model should be tested over a full range of angle of attack and at each incidence a full roll sweep should be done."¹ This would present the aircraft designer with quite a problem. Even after performing this very extensive test program, it would be no small task to extrapolate the results to full scale, considering the documented large effect of Reynolds number² and the known nonrepeatability of test results at high angles of attack. Fortunately, the indeterminate nature of the full-scale, high-alpha aerodynamics is eliminated by the so-called moving-wall effects.⁸

Presented as Paper 90-0067 at the 28th Aerospace Sciences Meeting, Reno, NV, Jan. 8-11, 1990; received Feb. 2, 1990; revision received Nov. 9, 1990; accepted for publication Dec. 10, 1990. Copyright © 1990 by Lars E. Ericsson. Published by the American Institute of Aeronautics and Astronautics, Inc., with permission.

*Retired; currently Engineering Consultant. Fellow AIAA.

The full-scale vehicle in free flight will only enter into the high-alpha regime when performing maneuvers, and the associated moving-wall effects will overpower the (static) effects of nose microasymmetries.² Even a modest body roll rate has a large effect on the developed side force,⁹ and the moving-wall effect generated by a coning motion is apparently equally powerful¹⁰ (Fig. 6). The authors of Ref. 10 described how only a slight push was needed to establish the coning motion in one direction or the other, regardless of the fact that the measured static yawing moment was biased in one direction due to nose microasymmetries.² The cone-cylinder model reached very nearly equal steady-state coning rates in positive and negative rotation directions. That is, the moving wall effects⁸ dominated over the static asymmetry, locking in the separation asymmetry in the direction of the body motion, driving it.

Analysis

In the case of a coning motion, the moving-wall effect acts in the following manner on the translating cross section (Fig.

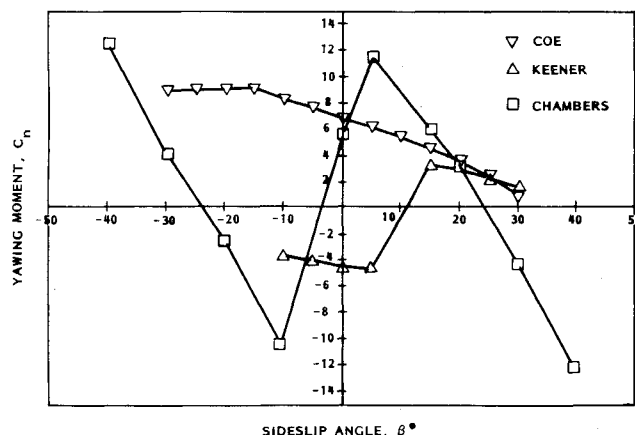


Fig. 1 Published $C_n(\beta)$ curves for ogive forebodies at $\alpha = 55$ deg.¹

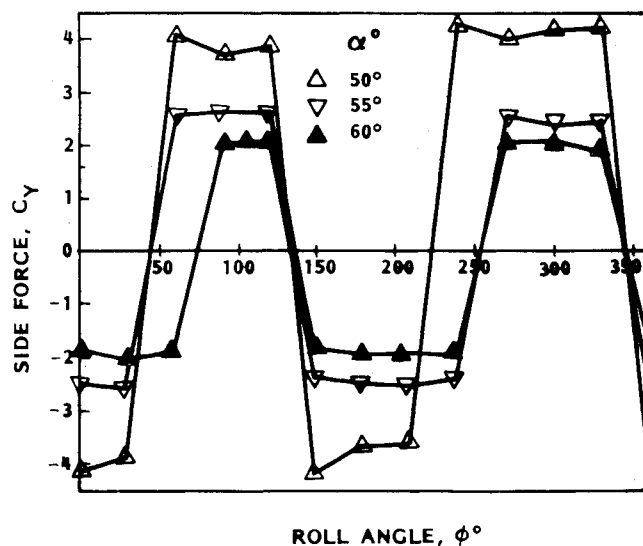


Fig. 2 $C_Y(\phi)$ characteristics of a 3.5-caliber ogive.¹

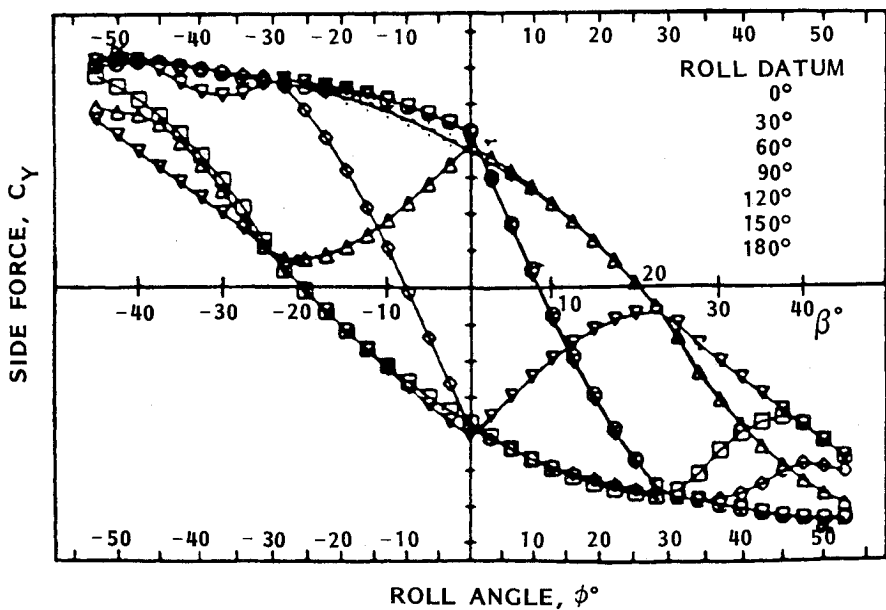


Fig. 3 Multiple solutions for $C_Y(\beta)$ of a 3.5-caliber ogive.¹

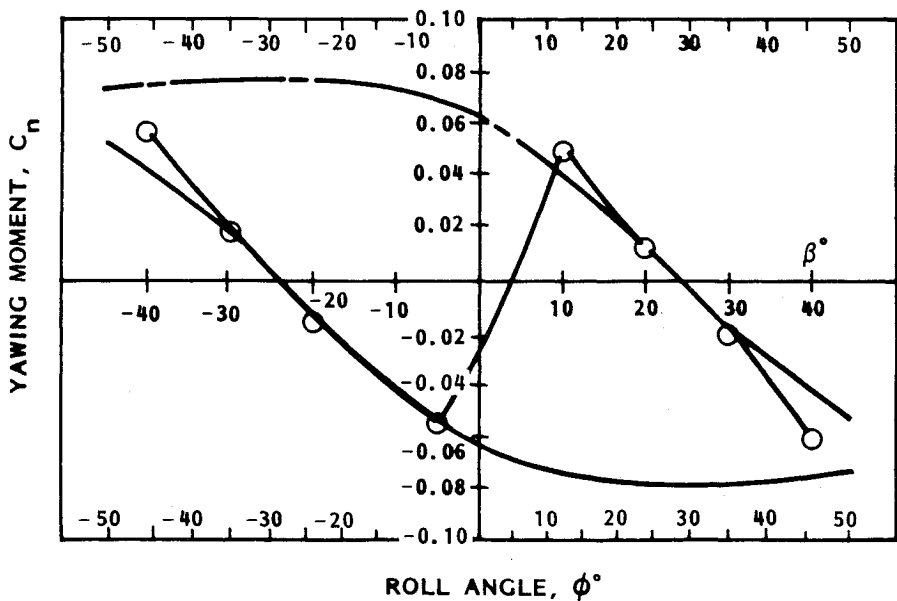


Fig. 4 Forebody contribution to $C_n(\beta)$ for the F-111 aircraft.¹

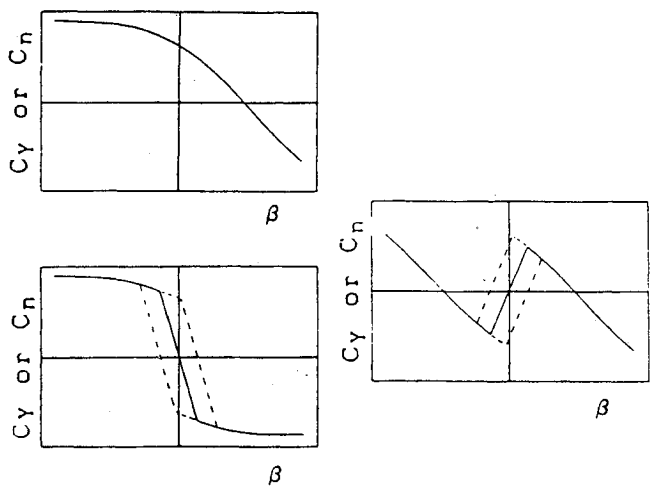


Fig. 5 Equally possible variations of $C_Y(\beta)$ and $C_n(\beta)$ characteristics.¹

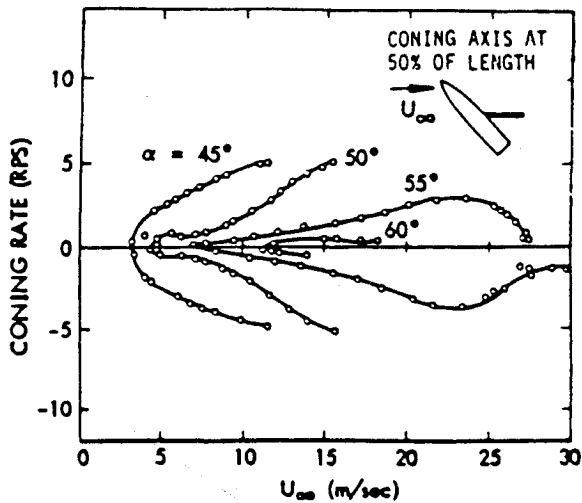


Fig. 6 Coning characteristics of cone-cylinder body.¹⁰

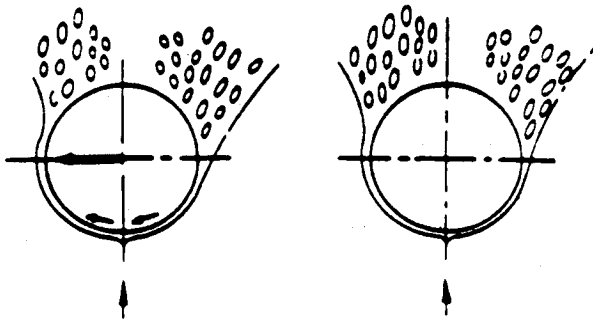
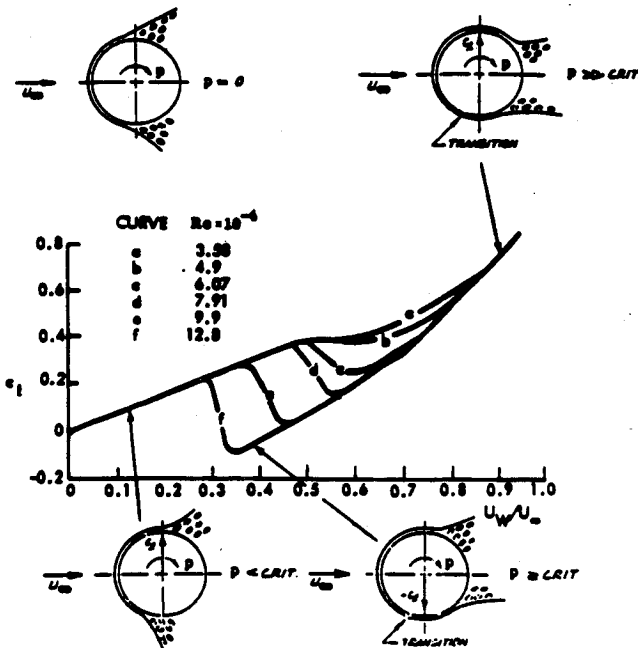


Fig. 7 Moving-wall effect on translating circular cross section.

Fig. 8 Magnus lift characteristics for initially subcritical flow conditions.¹³

7). The lateral motion of the circular cross section causes the flow separation to be delayed on the advancing side and promoted on the retreating side, the important moving-wall effects being those generated near the flow stagnation point.¹¹ Thus, the motion produces a force that drives it until an equilibrium coning rate is reached, where the separation-induced driving moment is balanced by the drag-generated damping moment.¹²

As it has been demonstrated² that the crossflow on a slender body becomes two dimensional in nature at $\alpha > 30$ deg, the moving-wall effects¹³ shown in Fig. 8 were used to define the moment that drives the coning motion. The damping moment was determined using the corresponding laminar drag characteristics, $c_d = 1.2$. The coning characteristics determined in this manner¹² give the prediction shown in Fig. 9. Aside from bearing friction effects, which were ignored in the analysis and would account for the needed finite magnitude of the velocity before the coning motion starts, the prediction agrees well with the experimental results.

The experimental results in Fig. 9 demonstrate that, during the initial spin up of the coning motion, the effect of roll angle shown in Fig. 2 is completely overpowered by the moving-wall effect. Consequently, on an advanced slender-nose aircraft performing a maneuver involving changes of roll and yaw, it is not the resulting effective sideslip β_{eff} that determines the separation asymmetry on the nose, as was assumed in Ref. 1, unless the sideslip is of significant magnitude. At moderate sideslip angles, it is instead the moving-wall effect that is

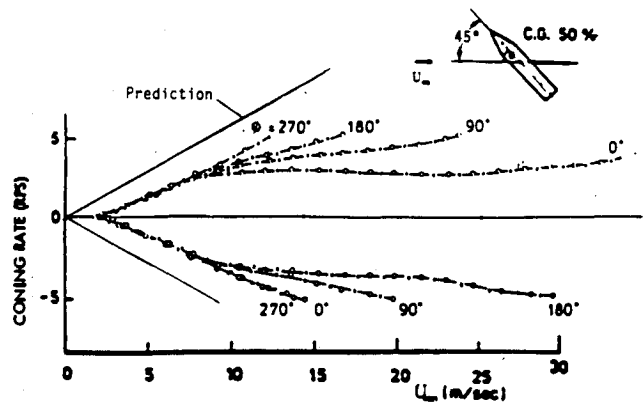


Fig. 9 Coning characteristics of pointed cone-cylinder body.

realized in the flow stagnation region on the nose that determines which way the side force, illustrated in Fig. 2, will flip.

Thus, the moving-wall effect present for the maneuvering full-scale vehicle will save the designer from the quandary illustrated by Figs. 5. However, the more or less discontinuous changes of C_Y and C_n , indicated by Figs. 5, could still cause aircraft control problems, and it may often be required to control the forebody flow asymmetry. The similarity between the moving-wall effect and the effect of a wall jet, discussed in Ref. 8, promises that control of the forebody separation asymmetry can be accomplished by much more subtle means than those tried so far.¹⁴

Conclusions

An examination of the high-alpha aerodynamics of slender-nose aircraft shows that the fickle effect of nose microasymmetries, giving erratic, highly nonlinear side-force and yawing moment characteristics in static tests, is overpowered by the moving-wall effect generated by the maneuvers performed by an aircraft when it enters the high-alpha flight regime.

References

- Lamont, P., and Kennaugh, A., "Multiple Solutions for Aircraft Sideslip Behavior at High Angles of Attack," AIAA Paper 89-0645, Jan. 1989.
- Ericsson, L. E., and Reding, J. P., "Asymmetric Vortex Shedding from Bodies of Revolution," *Tactical Missile Aerodynamics*, edited by M. J. Hemmich and J. N. Nielson, Vol. 104, Progress in Astronautics and Aeronautics, AIAA, New York, 1986, pp. 243-296.
- Coe, P. L., Jr., Chambers, J. R., and Letko, W., "Asymmetric Lateral-Directional Characteristics of Pointed Bodies of Revolution at High Angles of Attack," NASA TN D-7095, Nov. 1972.
- Keener, E. R., Chapman, G. T., Cohen, L., and Taleghani, J., "Side Forces on a Tangent Ogive Forebody with a Fineness Ratio of 3.5 at High Angles of Attack and Mach Numbers from 0.1 to 0.7," NASA TM X-3437, Feb. 1977.
- Grafton, S. B., Chambers, J. R., and Coe, P. L., Jr., "Wind-Tunnel Free-Flight Investigation of a Model of a Spin Resistant Fighter Configuration," NASA TN D-7716, June 1974.
- Malcolm, G. N., Ng, T. T., Lewis, L. C., and Murri, D. G., "Development of Non-Conventional Control Methods for High Angle of Attack Flight Using Vortex Manipulation," AIAA Paper 89-2192, Aug. 1989.
- Chambers, J. R., Anglin, E. L., and Bowman, J. S., Jr., "Effects of a Pointed Nose on Spin Characteristics of a Fighter Airplane Model Including Correlation With Theoretical Calculations," NASA TN D-5921, 1970.
- Ericsson, L. E., "Moving Wall Effects in Unsteady Flow," *Journal of Aircraft*, Vol. 25, No. 11, 1988, pp. 977-990.
- Atraghji, E. G., "The Influence of Mach Number, Semi-Nose Angle and Roll Rate on the Development of the Forces and Moments over a Series of Long Slender Bodies of Revolution at Incidence," National Research Council, NAE Data Rept. 5x5/0020, Ottawa, Canada, 1967.
- Yoshinaga, T., Tate, A., and Inoue, K., "Coning Motion of Slender Bodies at High Angles of Attack in Low Speed Flow," AIAA Paper 81-1899, Aug. 1981.

¹¹Ericsson, L. E., "Circular Cylinder Response to Karman Vortex Shedding," *Journal of Aircraft*, Vol. 25, No. 9, 1988, pp. 769-775.

¹²Ericsson, L. E., "Prediction of Slender Body Coning Characteristics," *Journal of Spacecraft and Rockets*, Vol. 28, No. 1, 1991, pp. 43-49.

¹³Swanson, W. M., "The Magnus Effect: A Summary of Investigations to Date," *Journal of Basic Engineering*, Vol. 83, No. 9, 1961, pp. 461-470.

¹⁴Ericsson, L. E., "Control of Forebody Flow Asymmetry, a Critical Review," AIAA Paper 90-2833, Aug. 1990.

Poststall Airfoil Response to a Periodic Freestream

Richard M. Howard* and David J. Gwilliam Jr.†
Naval Postgraduate School,
Monterey, California 93943

I. Introduction

THE maintenance of air superiority in the future will depend on an ability to perform rapid transient maneuvers at high angles of attack, often into the poststall flight regime. This new class of flight maneuvers will require a more complete understanding of high-alpha unsteady flight dynamics and aerodynamics. During a high angle-of-attack maneuver, any sudden unintentional asymmetry induced in the flow over the lifting surfaces could adversely affect the control of the aircraft. A change in the wing-boundary-layer behavior for an aircraft operating near stall or in the poststall regime may potentially affect the ability of the flow to remain attached during the maneuver—or to remain separated. This situation may arise when the lifting surface of a maneuvering aircraft penetrates the wake of a second aircraft, is disturbed by the blast from a launched missile, or receives adverse interference from the wake of a canard during an aggressive maneuver.

The effects of steady disturbances on airfoil boundary-layer behavior have been studied extensively; unsteady effects have been treated to a much lesser degree. Most research of an unsteady flowfield has involved either a pitching airfoil, related to dynamic stall,¹ or a streamwise velocity variation, usually sinusoidal, over a stationary wing section.² Bar-Sever³ introduced transverse velocity fluctuations upstream of an airfoil leading edge using an oscillating-wire technique; periodic forcing of the velocity field was shown to increase the static poststall lift coefficient by 38%. Howard and Miley⁴ observed the periodic response in a wing boundary layer immersed in a propeller slipstream and found a stabilizing mechanism to provide a time-dependent relaminarization over the airfoil. Renoud and Howard⁵ considered the case of the wing-boundary-layer response behind a spinning rod for attached flows and found the same mechanism to exist without any propeller thrusting. The current effort looks at the features of the two previous studies that involved the superposition of a periodic wake flow on a mean flowfield, but for a poststall flow regime. It was desired to determine if there exists a stabilizing influence on the separating flow. Understanding the response of such a flowfield may lead to unusual methods of control in the maneuvering high angle-of-attack flight regime.

Received Oct. 24, 1990; presented as Paper 91-0431 at the AIAA 29th Aerospace Sciences Meeting, Reno, NV, Jan. 7-10, 1991; revision received March 27, 1991; accepted for publication April 5, 1991. This paper is declared a work of the U.S. Government and is not subject to copyright protection in the United States.

*Assistant Professor, Department of Aeronautics and Astronautics Code AA/MO. Senior Member AIAA.

†Graduate Student, Weapons Engineering; Lieutenant, U.S. Navy; currently, Weapons Control Officer, USS Bunker Hill, 3750 Jennings Chapel Road, Woodbine, MD 21797.

II. Experimental Investigation

Tests were performed in the low-speed wind tunnel at the Naval Postgraduate School. This wind tunnel is of the closed-return type with a 32- \times 45-in. test section. A 2-ft wide, 10-in.-chord airfoil model was supported between vertical plates running from the floor to the ceiling. The wing section used was from a helicopter tail rotor, filled to contour and refinished. A 3/8-in.-diam polished steel rod 16 in. long was rotated 10% chord distance upstream of the wing leading edge, with the axis of rotation 25% chord distance below the chordline. The nominal test-section velocity U_∞ was maintained at 95 ft/s for a Reynolds number based on chord c of 5×10^5 . The ambient turbulence intensity at the test dynamic pressure was 0.18%.

To sense the flow reversal expected with the separated flowfield, a split-film probe was used. The split-film probe consists of two electrically independent nickel-film sensors placed on a quartz fiber yielding flow velocity and flow angle in the streamwise plane. Only one case studied will be presented here; complete results can be found in Ref. 6. Data were gathered at 3.53 kHz at a turbulent-pulse frequency ω (two pulses per rotation) of 3 Hz and a sampling time of 5.67 s for a reduced frequency $k = \omega \cdot c / (2 \cdot U_\infty)$ of 0.09. Seventeen turbulent pulses were recorded for ensemble averaging of phase-locked velocity profiles. A low-pass digital filter was applied by frequency-domain smoothing.

III. Results

Measurements were made at 22-deg angle of attack at the 70% chord position. Ensemble-averaged values of the total velocity V and the streamwise component u for the undisturbed case (no spinning rod) are shown in Fig. 1. The total velocity across the vertical dimension might be interpreted to be a boundary-layer profile, with a velocity level of 40–50% of U_∞ . The streamwise component, though, indicates that the profile is actually one of incipient separation, with little forward or reversed flow in this region near the surface.

Figure 2 shows ensemble time histories for the streamwise velocity component across the separated layer. The time t is

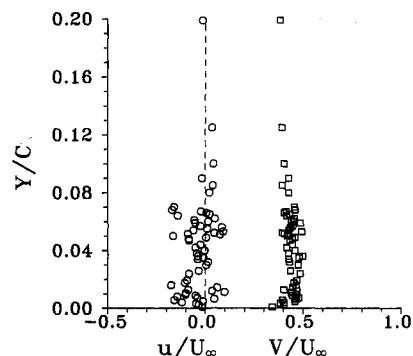


Fig. 1 Total and streamwise velocity profiles, 70% chord, $\alpha = 22$ deg, no disturbance input.

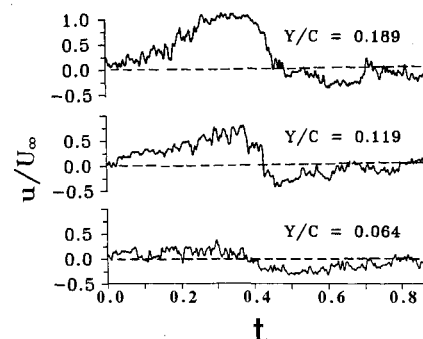


Fig. 2 Streamwise velocity time histories, 70% chord, $\alpha = 22$ deg, $k = 0.09$.